Accurate Fault Location Algorithm for Power Transmission Lines

J. Sadeh, A. M. Ranjbar, N. Hadjsaid, R. Feuillet

Abstract

In this paper we propose a new fault location algorithm for power transmission lines based on one terminal voltage and current data. A distributed time domain model of the line is used as a basis for algorithm development. The suggested technique only takes advantage of post-fault voltage and current samples taken at one end of the line and does not require filtering of DC offset and high-frequency components of the recorded signals, which are present during transient conditions. Another advantage of the proposed method is the application of a very narrow window of data i. e. less than 1/4 of a cycle. The paper also proposes two different algorithms for lossless and lossy line models. Computer simulations approved the accuracy of the proposed methods.

1 Introduction

Rapid detection, location and clearance of faults are essential factors of satisfactory operation of power supply networks. When a fault occurs on the transmission line of an electric power system, it is very important to find the exact location of the fault. This can result in reducing the time required for repairing the damage caused by the fault and consequently improving reliability and continuity of energy supply.

Fault location of transmission lines has always been a very well-known subject, being studied for a long time. However, this problem has nowadays been of more importance, due to deregulation and required quality of supply. Overhead lines in power systems have always been subject to faults, which can be either transient or permanent and can be caused by various reasons. In case of permanent faults, locating the fault point allows one to go to the exact location and to take appropriate actions to restore the power. In the case of transient faults – which are usually cleared by automatic reclosing systems – locating the fault permits identifying critical points in the system and taking the necessary preventative maintenance steps. These critical points may be caused by several reasons as pollution, insufficient insulation level, bird interference, etc.

Many techniques have been proposed and applied for locating the exact point of fault on transmission lines [1 – 14]. The main differences between these various algorithms are due to different transmission line models (lumped [1 – 3] or distributed [4 – 6]), and the data required (of one end [1, 4, 7] or two ends of the line [2, 8, 9]).

Sant and *Paithankar* [10] proposed a fault location algorithm technique that uses fundamental frequency voltage and current measured at one of the line terminals. This technique assumed that the line is connected to a source at one end only. The estimate of fault locations is not accurate if the fault current is supplied from both line terminals and some fault resistance is present. *Takagi* et al. [7], *Wiszniewski* [3], *Eriksson* et al. [1] and *Cook* [2] proposed methods which use fault current distribution factors, pre-fault and post-fault current and post-fault voltage from one line terminal. Impedances of equivalent sources connected to the line terminals are required. In practice, the system configuration changes from time to time modifying distribution factors. *Richards* and *Tan* [11] present a dynamic parameter estimation algorithm for locating faults, based on locally available currents and voltages. The differential equations are based on a lumped parameter line model. For modelling of the rest of the system at both ends of the line, Thevenin equivalents are utilised. The fault location problem is treated as a parameter estimation problem of a dynamic system, in which the response of the physical system is compared with the one of a lumped parameter model. The model parameters (location and resistance of the fault) are varied until an adequate match is obtained with the physical system response. The travelling wave approach was also studied [4 – 6, 12, 13]. This approach is based either on the travel time measurements using correlation technique [12] or on the calculation of voltages and/or currents profiles along the transmission line [4 – 6, 13]. The travelling wave techniques offer some advantages but the computational complexity is increased. Time domain representation of a transmission line model has also been considered [14]. The model is obtained using the Laplace and Z transforms. Data samples are considered as being available from one end only. The voltage at the other end is estimated using pre-fault data.

In calculating the distance to a fault point, using voltage and current signals, it is advantageous to use terminal data of both sides of the faulty transmission line. However, from the practical point of view, it is more appropriate that the algorithm uses only one terminal voltage and current data, which leads to simplicity of the equipment used.

This paper introduces a new fault location algorithm that needs one terminal post-fault data and uses distributed time-domain model of transmission line to achieve required accuracy. The idea of the introduced

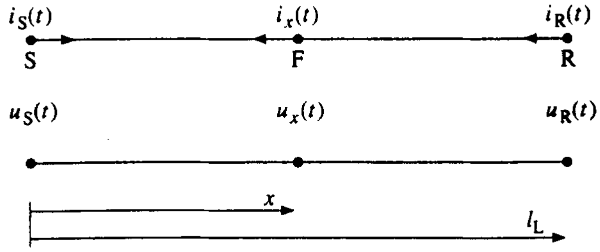

Fig. 1. Transmission line with distributed parameters

algorithm is that it considers fault location, as an optimization problem that can be solved by an appropriate mathematical method.

2 Distributed Model of Transmission Line

A single-phase model of a three-phase transmission line with distributed parameters is shown in **Fig. 1**. In this figure S represents the sending end and F is taken as an arbitrary point at a distance x ($x \le l_L$) from S along the line. The distributed model [15] of the SF segment is shown in **Fig. 2**.

The following equations can be derived according to this figure:

$$i_S(t) = \frac{1}{Z_c^*} u_S(t) + I_S(t-\tau), \tag{1}$$

$$i_x(t) = \frac{1}{Z_c^*} u_x(t) + I_x(t-\tau). \tag{2}$$

In these equations dependent current sources i. e. I_S and I_x are defined as:

$$I_S(t-\tau) = \frac{-R^*/4}{Z_c^{*2}}\left[u_S(t-\tau) + Z_c^{**} i_S(t-\tau)\right] - \frac{Z_c}{Z_c^{*2}}\left[u_x(t-\tau) + Z_c^{**} i_x(t-\tau)\right], \tag{3}$$

$$I_x(t-\tau) = \frac{-R^*/4}{Z_c^{*2}}\left[u_x(t-\tau) + Z_c^{**} i_x(t-\tau)\right] - \frac{Z_c}{Z_c^{*2}}\left[u_S(t-\tau) + Z_c^{**} i_S(t-\tau)\right], \tag{4}$$

where

τ time elapsed for the wave propagation from S to F,
Z_c characteristic (surge) impedance,
R^* line resistance from S to F,
$Z_c^* = Z_c + R^*/4$,
$Z_c^{**} = Z_c - R^*/4$.

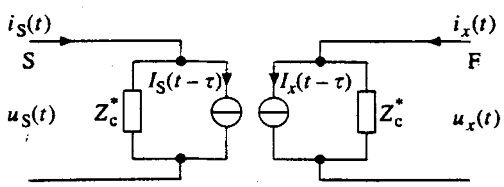

Fig. 2. Distributed model of the SF segment

As seen in eqs. (3) and (4), in the case where transmission line resistance is significant and is observed, the dependent current sources I_S and I_x are functions of voltages and currents at both sides of the line. When the line resistance is small enough to be ignored, eqs. (3) and (4) can be simplified as eqs. (5) and (6), while eqs. (1) and (2) remain unchanged:

$$I_S(t-\tau) = \frac{-1}{Z_c} u_x(t-\tau) - i_x(t-\tau), \tag{5}$$

$$I_x(t-\tau) = \frac{-1}{Z_c} u_S(t-\tau) - i_S(t-\tau). \tag{6}$$

These equations imply that unlike former case, the dependent current sources I_S and I_x are only a function of currents and voltages on the opposite side of the line. The algorithm will be developed applying these equations and data gathered from one side of the line.

3 Fault Location Algorithms

3.1 Mathematical Definition

Let $u_x(t)$ and $i_x(t)$ represent the voltage and current at point x on a transmission line. $u_x(t)$ and $i_x(t)$ satisfy the hyperbolic system of partial differential equations

$$\frac{\partial u}{\partial x} + L' \frac{\partial i}{\partial t} = -R' i, \tag{7}$$

$$C' \frac{\partial u}{\partial t} + \frac{\partial i}{\partial x} = 0, \tag{8}$$

where R', L' and C' are the resistance, inductance and capacitance per unit length of the line, respectively. Let the voltage at a fault point F on the line be given by

$$u_x(t) = u_F, \quad t \ge t_0, \tag{9}$$

where t_0 represents the instant when the fault occurs.

The voltage and current records at the local end of the line during the fault can be represented over time t by:

$$\begin{cases} u_S(t) \\ i_S(t) \end{cases} \quad t_0 \le t \le T + t_0, \tag{10}$$

where T is the window length of recording. The fault location problem can then be defined as follows:

- Determine the co-ordinate x by using the line model of eqs. (7) and (8) and the data set of eq. (10).

In order to solve this problem, two distinct cases are considered. One with a lossless line model and the other by taking the line resistance into consideration.

3.2 Lossless Transmission Line

Suppose that a solid short circuit ($u_F = 0$) has occurred at point F, at distance x from the sending end of the transmission line. According to the distributed time domain model of transmission line and considering eqs. (5) and (6), we obtain:

$$u_S(t) = Z_c i_S(t) + Z_c i_x(t-\tau) + u_x(t-\tau), \quad (11)$$

$$u_x(t) = Z_c i_x(t) + Z_c i_S(t-\tau) + u_S(t-\tau), \quad (12)$$

Without loss of generality, we suppose that the short circuit has occurred at $t_0 = 0$. In order to cancel the undetermined current i_x in eqs. (11) and (12), we shift eq. (11) by τ seconds. According to these equations and eq. (9) one can write:

$$u_S(t+\tau) + u_S(t-\tau) = Z_c\left(i_S(t+\tau) - i_S(t-\tau)\right). \quad (13)$$

The distance to the fault point x does not appear explicitly in eq. (13), and is hidden in the surge travelling time τ. Furthermore, τ does not appear as a variable in eq. (13), but as the value on which the voltage and current depend. Eq. (13) can be written in discrete form as

$$u_S(k+m) + u_S(k-m) = Z_c\left(i_S(k+m) - i_S(k-m)\right), \quad (14)$$

where

$m\Delta t = \tau$,
$k\Delta t = t$,
Δt sampling step,
m, k arbitrary integers.

Eq. (14) is available for each sample. Since there is only one unknown x, this equation is over-specified. The best estimate may be found based on the minimum least-square estimate technique. In this particular case, the criterion to be minimized is

$$J_1(m) = \sum_{k=m}^{N-m} \left[\frac{u_S(k+m) + u_S(k-m)}{i_S(k+m) - i_S(k-m)} - Z_c \right]^2, \quad (15)$$

where

N total number of samples ($N\Delta t = T$).

Since the criterion is not linearly dependent on m, the search for a minimum has to be performed in an approximate way. For this purpose the value of the criterion defined by eq. (15) is evaluated for different values of m. The minimum of these criterion values determines the final value of m for which the corresponding fault location is determined.

3.3 Lossy Transmission Line

This section describes an algorithm for solving the fault location problem for lossy transmission line. Similar to the previous case, we supposed that the short circuit is occurred at point F on the transmission line at a distance x from the sending end. According to eqs. (1) to (4) we obtain:

$$u_S(t) = Z_c^* i_S(t) + \frac{R^*/4}{Z_c^*}\left[u_S(t-\tau) + Z_c^{**} i_S(t-\tau)\right] + \frac{Z_c}{Z_c^*}\left[u_x(t-\tau) + Z_c^{**} i_x(t-\tau)\right], \quad (16)$$

$$u_x(t) = Z_c^* i_x(t) + \frac{R^*/4}{Z_c^*}\left[u_x(t-\tau) + Z_c^{**} i_x(t-\tau)\right] + \frac{Z_c}{Z_c^*}\left[u_S(t-\tau) + Z_c^{**} i_S(t-\tau)\right]. \quad (17)$$

Cancelling the undetermined parameter from the above equations leads to the following expression:

$$u_S(t+\tau) - Z_c^* i_S(t+\tau) + \frac{R^*/4}{Z_c^*}\left[\frac{Z_c^{**}}{Z_c^*}\left(u_S(t) - Z_c^* i_S(t)\right) - \left(u_S(t) + Z_c^{**} i_S(t)\right)\right] + \frac{Z_c^{**}}{Z_c^{*3}}\left(Z_c^2 - (R^*/4)^2\right)\left[u_S(t-\tau) + Z_c^{**} i_S(t-\tau)\right] = 0. \quad (18)$$

In this case, the unknown parameter x not only implicitly appears in the voltage and current argument, but also explicitly appears in the variables R^*, Z_c^* and Z_c^{**}. By discretizing the above equation we introduced:

$$F(m,k) = 0. \quad (19)$$

The F function is given in the **Appendix**. Eq. (19) is again over-specified since it has just one unknown variable distance x to the fault point. Therefore the best estimate may be found based on the minimum least-square estimate technique. In order to determine the location of the fault, the following optimization problem must be solved:

$$\min_m J_2(m) = \min_m \sum_{k=m}^{N-m} F^2(m,k). \quad (20)$$

4 Three-Phase Unbalanced Faults

The location of unbalanced faults can also be determined by using this method. The procedure is similar to the case of balanced faults.

In the case of unbalanced faults, firstly the coupled equations in the phase domain must be transformed into the decoupled equations in the modal domain. In regard to balanced lines, there are a number of simple transformation matrices, which decouple the line equations. For instance, such a matrix and its inverse for three-phase lines are [15]:

$$\boldsymbol{M} = \begin{bmatrix} 1 & 1 & 1 \\ 1 & -2 & 1 \\ 1 & 1 & -2 \end{bmatrix}, \quad \boldsymbol{M}^{-1} = \frac{1}{3}\begin{bmatrix} 1 & 1 & 1 \\ 1 & -1 & 0 \\ 1 & 0 & -1 \end{bmatrix}. \quad (21)$$

Using the inverse transformation matrix $\boldsymbol{M}^{-1}$, the sending end voltages in modal domain can be written as:

$$\begin{cases} u_S^0(t) = \left[u_S^{L1}(t) + u_S^{L2}(t) + u_S^{L3}(t)\right]/3, \\ u_S^1(t) = \left[u_S^{L1}(t) - u_S^{L2}(t)\right]/3, \\ u_S^2(t) = \left[u_S^{L1}(t) - u_S^{L3}(t)\right]/3. \end{cases} \quad (22)$$

After decoupling the system equations, we are able to apply the same procedure for each of the three modes, leading to Bergeron's equations for the three phase line.

5 Test Results

In this section the performance of the algorithms were evaluated. **Fig. 3** shows a 400-kV, 308-km long

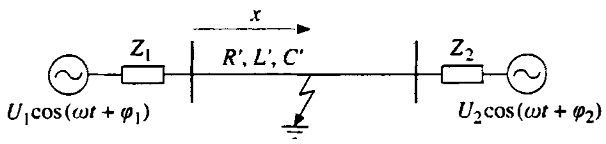

Fig. 3. Study system

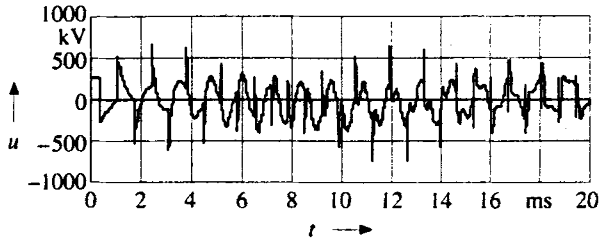

Fig. 4. Sending end voltage for 90° fault inception angle

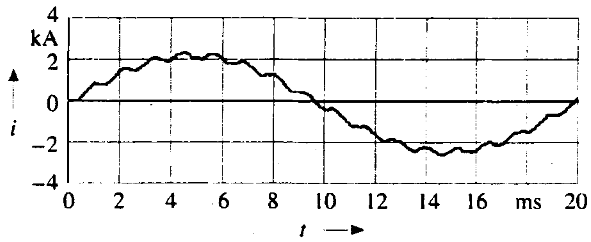

Fig. 5. Sending end current for 90° fault inception angle

three-phase transmission line with distributed parameters that are given in the **Appendix**. A three-phase fault occurs at an arbitrary point F at a distance x from sending end. For x equal to 100 km, the voltage and current of phase L1 at the sending end are shown in **Fig. 4** and **Fig. 5**, respectively. For this case the fault inception angle has been assumed to be 90°. These curves are obtained from MATLAB, and resemble the results from EMTP to a great extent.

For this condition, the criterion functions J_1 and J_2 are shown in **Fig. 6** versus distance d. The minima of these criterion functions determine the fault location in two cases, namely lossless and lossy transmission line. According to this figure, it is concluded that high accuracy in line model leads high accuracy in results. For calculation of criterion functions we applied only the post- fault voltage and current samples taken at the sending end of the line. These data do not require filtering of DC offset and high-frequency content. The data window used in the calculation contained 2.5 ms to 3.5 ms of post-fault data, starting from the fault occurrence.

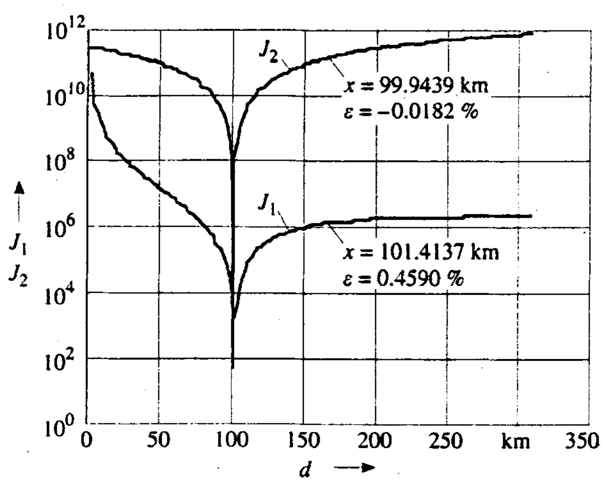

Fig. 6. Criteria functions J_1 and J_2 for fault at 100 km and 90° fault inception angle

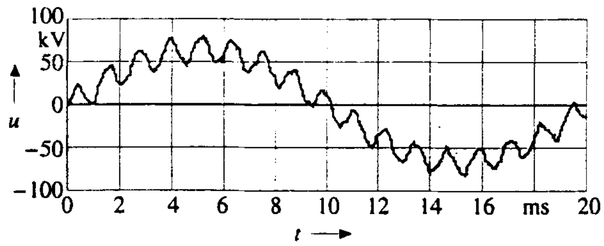

Fig. 7. Sending end voltage for zero fault inception angle

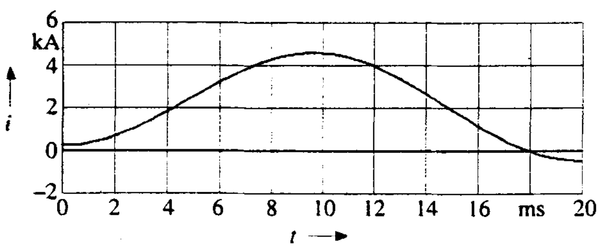

Fig. 8. Sending end current for zero fault inception angle

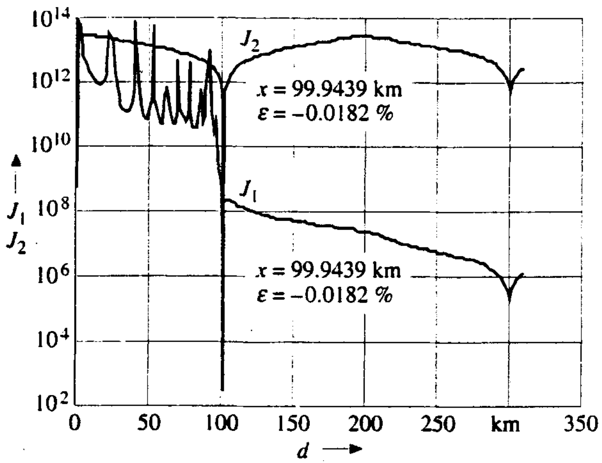

Fig. 9. Criteria functions J_1 and J_2 for fault at 100 km and zero fault inception angle

In order to analyse the accuracy of the algorithm at different fault situations, we performed extensive tests by various inception angles. As an instance, for zero fault inception angle, the voltage and current at the sending end for fault location at 100 km are shown in **Fig. 7** and **Fig. 8**, respectively. The criterion functions for this case are depicted in **Fig. 9**. The result was still satisfactory despite very large DC offset in current signal, as shown in Fig. 8.

To investigate the accuracy of the proposed methods for various fault locations, the percentage of error is plot-

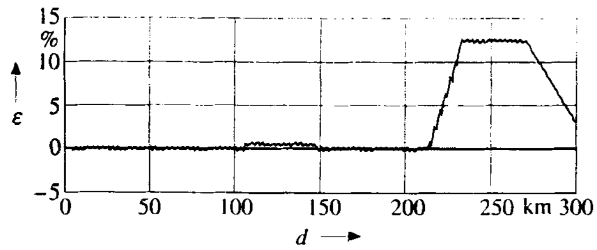

Fig. 10. Percentage of error for lossless line model

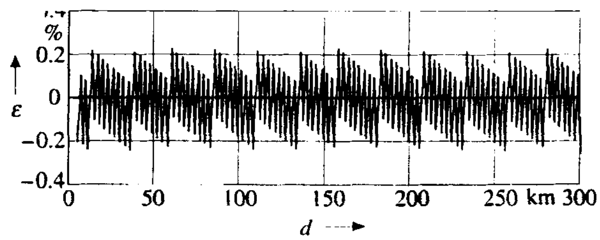

Fig. 11. Percentage of error for lossy line model

ted against fault distance in **Fig. 10** and **Fig. 11.** These figures are prepared for the case of a 45° inception angle. Fig. 10 and Fig. 11 involve the cases of lossless and lossy line models, respectively. As seen in Fig. 10, faults occurring near the end of the line cause unacceptable errors due to inaccurate line model, whereas the locations of the fault are calculated accurately when precise line model is used.

Note that percentage of error ε is calculated as

$$\varepsilon\,(\text{in }\%) = \frac{x_{\text{est}} - x_{\text{real}}}{l_{\text{L}}} \cdot 100, \tag{23}$$

where

x_{est} calculated location of fault,
x_{real} actual location of fault,
l_{L} length of transmission line.

The proposed algorithm can be applied in the case of unbalanced faults (single-phase to ground, double-phase to ground and double phase) too. This algorithm has been tested for different fault locations. The results indicate very small errors in any cases, regarding both the locations and the types of fault. The percentage of error as a function of fault distance, for the most common fault type, i. e. the single-phase to ground, is depicted in **Fig. 12.** The results of this study show that the errors for unbalanced faults are slightly greater than for the balanced ones.

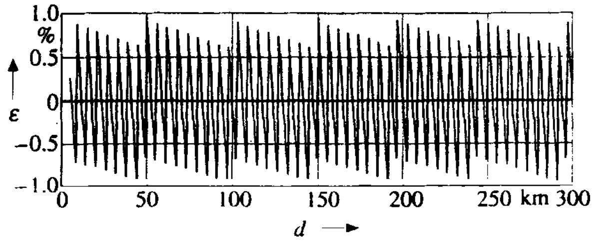

Fig. 12. Percentage of error for unbalanced fault

6 Conclusions

In this paper we proposed a new fault location algorithm using post-fault voltage and current samples taken at one end of the transmission line. The advantages claimed for this new algorithm are:

- No requirement for elimination of DC offset and high-frequency components of the data.
- Low sensitivity to fault inception angle and location of fault.
- High accuracy.
- Very narrow window of data (2.5 ms to 3.5 ms of post-fault data).

The algorithms were tested under a variety of simulated fault conditions. In the case of balanced faults, the estimated fault location errors were within 0.25 % line length for accurate model case while using the lossless (inaccurate) model lead to unacceptable errors specially when the fault occurs near the end of the line. But the results in the case unbalanced faults indicate that the estimated fault location errors were very small for all cases, as it never exceeds 1 %.

7 List of Symbols and Abbreviations

t	time
T	window length of recording
τ	time elapsed for the wave propagation from S to F
x	distance between F and S
Δt	sampling step
$i_{\text{S}}(t), u_{\text{S}}(t)$	sending end current and voltage
$i_{\text{R}}(t), u_{\text{R}}(t)$	receiving end current and voltage
$i_x(t), u_x(t)$	current and voltage of fault point
Z_{c}	characteristic (surge) impedance
R^*	line resistance from S to F
l_{L}	line length
R'	line resistance per unit length
L'	line inductance per unit length
C'	line capacitance per unit length
N	total number of samples
J_1, J_2	criterion functions
$\boldsymbol{M}$	transformation matrix
x_{est}	calculated location of fault
x_{real}	actual location of fault
EMTP	Electro-Magnetic Transient Program
F, R, S	fault point, receiving end, sending end

Appendix

A1 Function F

$$F(m,k) = u_{\text{S}}(k+m) - Z_{\text{c}}^{*} i_{\text{S}}(k+m) - \frac{R^{*}/4}{Z_{\text{c}}^{*}}\left[\frac{R^{*}/2}{Z_{\text{c}}^{*}} u_{\text{S}}(k) + 2 Z_{\text{c}}^{**} i_{\text{S}}(k)\right] + \frac{Z_{\text{c}}^{**2}}{Z_{\text{c}}^{*2}}\left[u_{\text{S}}(k-m) + Z_{\text{c}}^{**} i_{\text{S}}(k-m)\right] = 0. \tag{A1}$$

A2 Transmission-Line Data

Positive sequence	Zero sequence
$R'^{+} = 0.01537\ \Omega/km$	$R'^{0} = 0.04612\ \Omega/km$
$L'^{+} = 0.8858$ mH/km	$L'^{0} = 2.6574$ mH/km
$C'^{+} = 13.065$ nF/km	$C'^{0} = 4.355$ nF/km

References

[1] *Eriksson, L.; Saha, M. M.; Rockefeller, G. D.:* An accurate fault locator with compensation for apparent reactance in the fault resistance resulting from remote-end infeed. IEEE Trans. on Power Appar. a. Syst. PAS-104 (1985) no. 2, pp. 424–436

[2] *Cook, V.:* Fundamental aspects of fault location algorithms used in distance protection. IEE Proc. C-133 (1986) no. 6, pp. 359–368

[3] *Wiszniewski, A.:* Accurate fault impedance locating algorithm. IEE Proc. C-130 (1983) no. 6, pp. 311–314

[4] *Kohlas, J.:* Estimation of fault locations on power lines. 3rd IFAC Sympos., Hague/Delft, Netherlands 1973, Proc. pp. 393–402

[5] *Ibe, A. O.; Cory, B. J.:* A travelling wave-based fault locator for two- and three-terminal networks. IEEE Trans. on Power Delivery PWRD-1 (1986) no. 2, pp. 283–288

[6] *Ranjbar, A. M.; Shirani, A. R.; Fathi, A. F.:* A new approach for fault location problem on power lines. IEEE Trans. on Power Delivery PWRD-7 (1992) no. 1, pp. 146–151

[7] *Takagi, T.; Yamakoshi, Y.; Yamamura, M.; Kondow, R.; Matsushima, T.:* Development of a new type fault locator using one-terminal voltage and current data. IEEE Trans. on Power Appar. a. Syst. PAS-101 (1982) pp. 2892–2898

[8] *Kezunovic, M.; Mrkic, J.; Perunicic, B.:* An accurate fault location algorithm using synchronized sampling. Electric Power Syst. Res. 29 (1994) pp. 161–169

[9] *Novosel, D.; Hart, D. G.; Udren, E.; Garitty, J.:* Unsynchronized two-terminal fault location estimation. IEEE Trans. on Power Delivery PWRD-11 (1996) no. 1, pp. 130–138

[10] *Sant, M. T.; Paithankar, Y. G.:* Online digital fault locator for overhead transmission line. Proc. IEE 126 (1979) no. 11, pp. 1181–1185

[11] *Richards, G. G.; Tan, O. T.:* An accurate fault location estimator for transmission lines. IEEE Trans. on Power Appar. a. Syst. PAS-101 (1982) no. 4, pp. 945–950

[12] *Paithankar, Y. G.; Sant, M. T.:* A new algorithm for relaying and fault location based on auto-correlation of travelling waves. Electric Power Syst. Res. 8 (1984/1985) pp. 179–185

[13] *Ibe, A. O.; Cory, B. J.:* Fault location algorithm for multiphase power lines. IEE Proc. C-134 (1987) no. 1, pp. 43–50

[14] *Lawrence, D. J.; Waser, D. L.:* Transmission line fault location using digital fault recorders. IEEE Trans. on Power Delivery PWRD-3 (1988) no. 2, pp. 496–502

[15] *Dommel, H.:* Digital computer solution of electromagnetic transient in single and multi phase networks. IEEE Trans. on Power Appar. a. Syst. PAS-98 (1969) no. 4, pp. 388–399

Manuscript received on April 19, 1999

The Authors

Javad Sadeh (1968) received the BSc and MSc both in Electrical Engineering from Ferdowsi University of Mashhad, Mashhad, Iran in 1990 and 1994, respectively. Since 1995 he has been studying toward PhD degree in the Electrical Department of Sharif University of Technology, Tehran, Iran with the collaboration of the electrical engineering laboratory of the Institut National Polytechnique de Grenoble (INPG), France. His research interests are power-system protection, power-system dynamics and operation. (Sharif University of Technology, Dept. of Electrical Engineering, POB 11365-9363, Tehran, Iran, Phone: +98 21 600 53 17, Fax: +98 21 601 95 68, E-mail: Jsadeh@nri.ac.ir)

Ali Mohammad Ranjbar (1943) received the MSc Degree from Tehran University in 1967 and the PhD degree from Imperial College of London University in 1975. Since then he has been teaching at Sharif University of Technology Tehran, Iran, and currently he is a professor. He is Director of Niroo Research Institute since 1996 too. His research interests are power-system protection and electrical machine. (Sharif University of Technology, Dept. of Electrical Engineering, POB 11365-9363 , Tehran, Iran, Phone: +98 21 600 53 17, Fax: +98 21 601 95 68, E-mail: Ranjbar@rose.ipm.ac.ir)

Nouredine Hadjsaid (1964) received the Engineer degree in Electrical Engineering from the University of Tizi Ouzou, Algeria, in 1987, the "Diplome d'Etude Approfondies" and the "Doctoral de l'INPG" degree from the Institut National Polytechnique de Grenoble (INPG), France, in 1988 and 1992. Since 1993 he served as a associate professor at the Ecole National Superieure d'Ingenieur Electriciens de Grenoble and at the Laboratoire d'Electrotechnique de Grenoble (LEG). In 1998, he received the degree of "Habilitation a Diriger des recherches" from the same institute. His research interests are power-system operation and security. (Laboratoire d'Electrotechnique de Grenoble, BP 46, 38402 Saint Martin d'Heres, France, Phone: +33 476 82 71 52, Fax: +33 476 82 63 00, E-mail: Nouredine.Hadjsaid@leg.ensieg.inpg.fr)

Rene Feuillet (1953) received his Diplome d'Ingenieur and his Dr. Eng. degree in Electrical Engineering from National Polytechnic Institute of Grenoble (INPG), France, in 1976 and 1979, respectively. In 1991, he received the degree of "Habilitation a Diriger des recherches" from the same institute. From 1979 to 1998, he has been appointed as Assistant Professor at the National Electrical Engineering School of Grenoble (ENSIEG), France, and since 1998 he served as a full professor at the same institute. His research activities in the Grenoble Electrotechnical Laboratory (LEG) include modelling of power electronics converters and interference perturbations on power networks and components. (Laboratoire d'Electrotechnique de Grenoble, BP 46, 38402 Saint Martin d'Heres, France, Phone: +33 476 82 63 85, Fax: +33 476 82 63 00, E-mail: Rene.Feuillet@ensieg.inpg.fr)